ring in 1. Coordination of the Lewis-acid $W(CO)_5$ adducts to $W(CO)_4P_4$ in the molecular species (1) results in two significant changes: (1) the energies of the MOs associated with $W(CO)_4P_4$ are lowered somewhat due to partial orbital mixing with appropriate $W(CO)_5$ orbitals; (2) the W–CO bonding orbitals and tungsten 5d AOs for the four $W(CO)_5$ adducts are the main contributors to the higher energy bonding MOs (including the HOMOs) of 1. Thus, the HOMOs of 1 consist of essentially noninteracting $W(CO)_5$ orbitals. As with the $W(CO)_4P_4$ fragment per se, all orbitals with significant P_4 ring bonding contributions are completely filled, and there is no apparent reason for a P_4 ring distortion to occur. The doubly degenerate LUMOs, which are 4.0 eV higher in energy than the HOMOs, are effectively unchanged in orbital character upon going from $W(CO)_4P_4$ to 1. Although the molecular orbital diagram for 1 does not explain the P_4 ring distortion detected via the ^{31}P NMR data, it is consistent with the lack of reversible electrochemical behavior for 1.

Acknowledgment. This research was generously supported by the National Science Foundation (Grants CHE-8616697 and CHE-9013059). We are most grateful to Dr. Robert Weller (EXTREL FTMS, 8416 Schroeder Rd, Madison, WI 53711) for obtaining LD/FT mass spectra with an EXTREL FTMS-2000 spectrometer. We also thank Ms. Lori Petrovich, Mr. Jackson C. K. Ma, and Ms. Agnes Lee Ma (UW—Madison) for their assistance in obtaining additional ^{31}P and ^{13}C NMR spectra.

Registry No. 1, 136782-25-7; $1\cdot CH_2Cl_2$, 136782-26-8; $W(CO)_6$, 14040-11-0; P_4, 10544-46-4.

Supplementary Material Available: Figures providing the solution and solid-state ^{31}P NMR spectra and tables listing anisotropic displacement coefficients for $W_5(CO)_{24}P_4\cdot CH_2Cl_2$ under *P4nc* symmetry, atomic coordinates, anisotropic displacement coefficients, and selected bond lengths and angles for $W_5(CO)_{24}P_4\cdot CH_2Cl_2$ under *I*4 symmetry, and ion-peak assignments for the LD/FT mass spectra of $W_5(CO)_{24}P_4$ (7 pages); tables of observed and calculated structure factor amplitudes for $W_5(CO)_{24}P_4\cdot CH_2Cl_2$ under *P4nc* and *I*4 symmetry (10 pages). Ordering information is given on any current masthead page.

Synthesis, Stereophysical-Bonding Features, and Chemical–Electrochemical Reactivity of Two Dimetal-Bridging Diphosphide Complexes: $Co_2(\eta^5\text{-}C_5Me_5)_2(\mu_2\text{-}\eta^2\text{-}P_2)_2$ and $Fe_2(\eta^5\text{-}C_5Me_5)_2(\mu_2\text{-}\eta^2\text{-}P_2)_2$

Mary E. Barr[1] and Lawrence F. Dahl*

Department of Chemistry, University of Wisconsin—Madison, Madison, Wisconsin 53706

Received March 5, 1991

Two dimetal-bridging diphosphido complexes, $Co_2Cp^*_2(\mu_2\text{-}\eta^2\text{-}P_2)_2$ (1) and $Fe_2Cp^*_2(\mu_2\text{-}\eta^2\text{-}P_2)_2$ (2) ($Cp^* = \eta^5\text{-}C_5Me_5$), were synthesized by cophotolysis of P_4 with $CoCp^*(CO)_2$ and $Fe_2Cp^*_2(CO)_2(\mu_2\text{-}CO)_2$, respectively. 1 and 2 were characterized from X-ray diffraction, laser-desorption FT mass spectrometric, spectroscopic (^1H, ^{31}P NMR; IR), and electrochemical measurements. An X-ray diffraction study unambiguously showed that the 36-electron cobalt dimer (1) consists of two 14-electron CoCp* fragments linked at a nonbonding Co···Co distance of 3.10 Å by two four-electron-donating η^2-coordinated P_2 ligands. The X-ray crystallographic investigation of the corresponding 34-electron iron dimer (2) disclosed two FeCp* fragments separated by an electron-pair Fe–Fe distance of 2.59 Å; unfortunately, a rotational-type crystal disorder was encountered, which prevented a definitive determination of the number and bonding modes of the bridging phosphorus atoms from the crystallographic analysis per se. However, the X-ray data and a comparative analysis of mass spectral and ^{31}P NMR data for 1 and 2 provide persuasive evidence that the stoichiometry and connectivities of the phosphorus atoms in 2 are identical to those in 1. Cyclic voltammograms indicated that each dimer exhibits reversible oxidative behavior. Preliminary investigations of the potential chemical reactivities of these metal-bridged diphosphide ligands with H_2 and C_2H_4 revealed that they are relatively inert compared to the reactivities previously reported for metal-bridged disulfide ligands with these reagents.

Introduction

As part of our investigations[2] into the photolytic generation of organometallic phosphido complexes, we present herein the photochemical syntheses and characterizations of $Co_2Cp^*_2(\mu_2\text{-}\eta^2\text{-}P_2)_2$ (1) and $Fe_2Cp^*_2(\mu_2\text{-}\eta^2\text{-}P_2)_2$ (2) (where Cp* denotes $\eta^5\text{-}C_5Me_5$). These compounds were prepared from reactions of elemental P_4 with $CoCp^*(CO)_2$ and $[FeCp^*(CO)_2]_2$, respectively. While other organometallic diphosphide complexes are known,[3] 1 and 2 are of particular interest for two reasons. First, the structural elucidation of the mode of coordination of the four bridging phosphorus atoms in the (pentamethylcyclopentadienyl)cobalt dimer (1) as two η^2-P_2 ligands clarifies the previously reported ambiguous crystallographic evidence that its (tetramethylethylcyclopentadienyl)cobalt analogue may contain a *cyclo*-P_4 ligand.[3b,4] Second, isolation of 1 and 2 in our laboratory afforded the opportunity to instigate preliminary investigations into the chemical reactivity of metal-bridged diphosphide ligands toward

(1) Present address: Los Alamos National Laboratory, University of California, Los Alamos, NM 87545.

(2) (a) Barr, M. E.; Adams, B. R.; Weller, R. R.; Dahl, L. F.; *J. Am. Chem. Soc.* **1991**, *113*, 3052. (b) Barr, M. E.; Smith, S. K.; Spencer, B.; Dahl, L. F. *Organometallics*, preceding paper in this issue.

(3) (a) DiViara, M.; Stoppioni, P.; Peruzzini, M. *Polyhedron* **1987**, *6*, 351 and references therein. (b) Scherer, O. J. *Comments Inorg. Chem.* **1987**, *6*, 1. (c) Scherer, O. J. *Angew. Chem., Int. Ed. Engl.* **1985**, *24*, 924.

(4) Scherer, O. J.; Swarowsky, M.; Wolmershäuser, G. *Angew. Chem., Int. Ed. Engl.* **1988**, *27*, 405.

0276-7333/91/2310-3991$02.50/0

common molecular species, specifically H_2 and C_2H_4; this study was primarily motivated by the intriguing reactivity of such reagents with similar metal-bridged disulfide ligands.[5-8]

In a recent communication on the thermolytic synthesis and stereochemical characterization of $Rh_2(\eta^5\text{-}C_5Me_4Et)_2(\mu_2\text{-}\eta^2\text{-}P_2)_2$, Scherer et al.[4] mentioned (without giving any structural details) that a crystallographic analysis of the analogous cobalt complex had been performed. One of the two crystallographically independent $Co_2(\eta^5\text{-}C_5Me_4Et)_2P_4$ molecules was described as containing a P_4 bridging ligand coordinated as a "long" rectangle (with two short and two long sides), while the four phosphorus atoms of the other independent molecule appeared to be linked to both $Co(C_5Me_4Et)$ fragments a a "short" rectangle with nearly equivalent phosphorus distances. Each of these two hypothesized *cyclo*-P_4 units had an average P–P distance of 2.38 Å. No comment was made concerning this highly unusual occurrence of two stoichiometically equivalent dimers with markedly different P–P bonding in the same crystal.

On the basis of a crystallographic analysis of our corresponding photosynthetically obtained $Co_2Cp^*_2(\mu_2\text{-}\eta^2\text{-}P_2)_2$ (1), which conclusively shows the existence of the two separate η^2-P_2 bridging groups in the single crystallographically independent molecule, we proposed that the four electron-density peaks corresponding to the presumed *cyclo*-P_4 ring in the C_5Me_4Et-containing dimer are probably due to a resulting averaged structure involving two crystal-disordered orientations of the two P_2 ligands.[9] An analogous rotational-type disorder is reported here in the crystal structure of the closely related 34-electron $Fe_2Cp^*_2(\mu_2\text{-}\eta^2\text{-}P_2)_2$ (2). Although this crystal disorder precludes a definitive determination from the X-ray diffraction study per se of the number of phosphorus atoms and their bonding interactions, convincing evidence that the stoichiometry and connectivities of the bridging phosphorus atoms in 2 are identical with those in 1 is provided by a comparative mass spectral analysis combined with the crystallographic and ^{31}P NMR data.

The two dimeric systems, 1 and 2, are the first such compounds generated via photolytic dissociation of P_4 to P_2 units. A thought-provoking feature of these transition-metal bare-phosphido complexes is that the μ_2-P_2 ligand is structurally similar to the μ_2-S_2 ligand found in the molybdenum–sulfur $Mo_2Cp''_2(\mu_2\text{-}S_2)(\mu_2\text{-}S)_2$ dimers (where Cp″ denotes either η^5-C_5H_4Me or η^5-C_5Me_5),[5] which are involved in highly intriguing catalytic hydrogenolysis processes. Activation of dihydrogen via its coordination to the disulfide ligand of these two dimers yields the corresponding $Mo_2Cp''_2(\mu_2\text{-}SH)_2(\mu_2\text{-}S)_2$ dimers, which are detected intermediates in a number of hydrogenolysis reactions[6,7] including the reduction of SO_2 to S_8 and H_2O, RN=NR′ to RNH—NHR, RNO_2 to RNH_2, RCH=NR to RCH_2—NHR, and HC≡CH or H_2C=CH_2 to H_3C—CH_3. While a number of μ_2-S_2 transition-metal complexes are known, only the molybdenum complexes exhibit such diverse, facile catalytic behavior. In a recent comprehensive review, Rakowski DuBois[8] attributes the versatility of these molybenum–sulfide dimers to the strong Mo–S bonds, which stabilize the complexes against fragmentation, and to the abilities of the disulfide ligand and the metal centers to participate in favorable redox chemistry.

Both the cobalt dimer (1) and the iron dimer (2) exhibit reversible oxidative behavior, and the mass spectral data of 2 suggest that this iron dimer is reasonably robust to fragmentation into monomeric iron species. Therefore, it was deemed desirable to investigate whether the diphosphide ligands in 1 and 2 undergo simple addition of dihydrogen and of ethylene under reaction conditions (viz., room temperature, 1 atm of gas)[7b] similar to those required for these molecules to add to the bridging sulfide ligands of $Mo_2Cp''_2(\mu_2\text{-}S_2)(\mu_2\text{-}S)_2$. The results of these attempted reactions are presented and discussed herein.

Experimental Section

(a) General Procedures. All reactions, sample transfers, and manipulations were performed with oven-dried standard Schlenk-type glassware under a nitrogen atmosphere, either on a vacuum line, in a polyethylene glovebag, or in a Vacuum Atmospheres drybox. The following solvents were dried and distilled prior to use: CH_3CN ($CaSO_4$), THF (K/benzophenone), CH_2Cl_2 (CaH_2), toluene (sodium), and hexane (Skelly B cut, CaH_2). $[FeCp^*(CO)_2]_2$ and $CoCp^*(CO)_2$ were prepared by minor modifications of the standard preparations[10] of their cyclopentadienyl analogues. P_4 (Strem) and H_2 and C_2H_4 (Matheson) were used without further purification.

Solution infrared spectra were recorded on a Beckman 4240 spectrophotometer. ^{31}P NMR spectra were obtained with a Bruker WP-270 spectrometer. Electrochemical data were collected on a BAS-100 electrochemical analyzer with the cell enclosed in a nitrogen-filled Vacuum Atmospheres glovebox. Electrochemical solutions consisted of ca. 7 mL of solvent consisting of ca. 10^{-3} M compound and 0.1 M $[NBu_4]^+[PF_6]^-$ electrolyte. The working electrode was a platinum disk, the auxilliary electrode a platinum coil, and the reference electrode a Vycor-tipped aqueous SCE separated from the test solution by a Vycor-tipped salt bridge (0.1 M $[NBu_4]^+[PF_6]^-$ in CH_3CN). An *iR* compensation for solution resistance[11] was made before each current–voltage measurement was taken.

Mass spectra were obtained with an EXTREL FTMS-2000 Fourier transform (FT) mass spectrometer equipped with a 3.0-T superconducting magnet, an EXTREL laser desorption (LD) interface, and a Tachisto 215G pulsed infrared CO_2 laser. Additional details of the LD-FTMS instrument and procedures for data collection are given elsewhere.[9,12]

(b) Preparation and Physical Properties of $Co_2Cp^*_2P_4$ (1). In a typical reaction, $CoCp^*(CO)_2$ (0.68 g; 2.7 mmol) and an excess of P_4 (0.74 g; 24 mmol of P) were each dissolved in ~100 mL of toluene, and the solution was transferred to a water-cooled Pyrex photolysis apparatus equipped with a Hanovia 450-W medium-pressure Hg-vapor lamp. The mixture was irradiated at room temperature until the solution was a deep reddish brown and IR spectra indicated that much of the starting monomer was consumed (approximately 1.5 h). The solvent was removed overnight under a N_2 purge. The resulting solid was extracted (3×) with hexane and chromatographed on a 1.5 (width) × 20 (length) cm silica gel column (Bio-sil A, 200–325 mesh) packed with hexane. Unreacted P_4 and $CoCp^*(CO)_2$ were eluted with the solvent front, followed by the bluish purple 1 (0.04 g; 7.4% yield after recrystallization) and green $[CoCp^*(\mu_2\text{-}CO)]_2$.[13] The major product from this reaction was a red-brown toluene-soluble matrial, which remains uncharacterized.

1 is an air-sensitive compound which is soluble to some extent in all common organic solvents. An infrared spectrum of 1 in

(5) (a) Rakowski DuBois, M.; DuBois, D. L.; van Derveer, M. C.; Haltiwanger, R. C. *Inorg. Chem.* **1981**, *20*, 3064. (b) Brunner, H.; Meier, W.; Wachter, J.; Guggolz, E.; Zahn, T.; Ziegler, M. L. *Organometallics* **1982**, *1*, 1107.

(6) Kubas, G. J.; Ryan, R. R. *J. Am. Chem. Soc.* **1985**, *107*, 6138.

(7) (a) Casewit, C. J.; Coons, D. E.; Wright, L. L.; Miller, W. K.; Rakowski DuBois, M. *Organometallics* **1986**, *5*, 951. (b) Rakowski DuBois, M.; van Derveer, M. C.; DuBois, D. L.; Haltiwanger, R. C.; Miller, W. K. *J. Am. Chem. Soc.* **1980**, *102*, 7456.

(8) Rakowski DuBois, M. *Chem. Rev.* **1989**, *89*, 1.

(9) Bjarnason, A.; DesEnfants, R. E.; Barr, M. E.; Dahl, L. F. *Organometallics* **1990**, *9*, 657.

(10) (a) Brunner, H. *J. Organomet. Chem.* **1968**, *14*, 173. (b) Calderon, J. L.; Fontana, S.; Frauendorfer, E.; Day, V. W.; Iske, S. D. A. *J. Organomet. Chem.* **1974**, *64*, C16.

(11) He, P.; Avery, J. P.; Faulkner, L. R. *Anal. Chem.* **1982**, *54*, 1313A.

(12) Bjarnason, A. *Rapid Commun. Mass Spectrom.* **1989**, *3*, 373.

(13) Cirjak, L. M.; Ginsburg, R. E.; Dahl, L. F. *Inorg. Chem.* **1982**, *21*, 940.

hexane exhibits an absorption band at 1380 cm^{-1} assigned to the Cp* C–C stretches. A ^{31}P NMR spectrum (109.3 MHz; $CDCl_3$; 300 K; H_3PO_4 ext) shows a broad singlet ($w_{1/2}$ = 30 Hz) at δ –6.06 ppm. Both positive- and negative-ion LD-FTMS spectra[9] of 1 show similar fragmentation patterns. Signals found in both spectra include the parent-ion peak at m/z 512 ($[M]^{+,-}$) as well as fragment-ion peaks at m/z 543 ($[M+P]^{+,-}$), 497 ($[M - CH_3]^{+,-}$), 481 ($[M - P]^{+,-}$, 100%), and 450 ($[M - 2P]^{+,-}$).

(c) Preparation and Physical Properties of $Fe_2Cp^*_2P_4$ (2). The iron dimer (2) was synthesized and purified by a procedure similar to that used to generate 1. Typically, $[FeCp^*(CO)_2]_2$ (0.95 g; 1.92 mmol) was reacted with an excess of P_4 (0.63 g; 20 mmol of P) in ~200 mL of toluene. Photolysis at room temperature for 2–2.5 h produced a dark brown solution. Extraction with hexane (3×) followed by chromatographic separation of this extract yielded the following complexes: green $FeCp^*P_5$[14] (0.13 g; 10% yield) eluted with hexane, yellow-brown 2 (0.04 g; 4% yield) eluted with 1:1 hexane/toluene, and traces of unreacted $[FeCp^*(CO)_2]_2$. As with the cobalt reaction, the majority of the products of this reaction remain uncharacterized.

2 is a highly air-sensitive compound. It is soluble in a variety of solvents including hexane, methylene chloride, and acetone. A solution IR spectrum of 2 in hexane shows one Cp* absorption band at 1372 cm^{-1}. A ^{31}P NMR spectrum (109.3 MHz; $CDCl_3$; 300 K; H_3PO_4 ext) consists of a broad singlet ($w_{1/2}$ = 38 Hz) at δ 126.58 ppm. Both positive- and negative-ion LD-FTMS spectra[9] show the parent-ion peak at m/z 506 ($[M]^{+,-}$) corresponding to the most abundant fragment. Other positive-ion peaks are observed at m/z 475 ($[M - P]^+$), 444 ($[M - 2P]^+$), and 326 ($[Cp^*_2Fe]^+$). Negative-ion fragment peaks include those at m/z 491 ($[M - CH_3]^-$), 475 ($[M - P]^-$), 371 ($[M - Cp^*]^-$), and 315 ($[M - FeCp^*]^-$).

(d) Attempted Addition of C_2H_4 and H_2 to $Co_2Cp^*_2P_4$ (1) and $Fe_2Cp^*_2P_4$ (2). Approximately 0.02 g of 1 was dissolved in 20 mL of 1:1 toluene/hexane, and the mixture was let to stir with C_2H_4 slowly bubbling through the solution. When no visible change occurred within $^1/_2$ h, the solution was allowed to stir under 20 psi of C_2H_4 for an additional 1 h. No visual or IR-detectable evidence of any reaction was observed. The solution containing 1 was then put through a single freeze/pump/thaw cycle to remove C_2H_4, and the procedure was repeated with H_2(g) as the potential reactant. Again, there was no detectable change in 1. Chromotography of the reaction mixture on silica, as outlined above, confirmed that the only compound present was unreacted 1.

Similar reactions were attempted with ca. 0.02 g of 2 in 20 mL of THF. Although the reaction times were doubled, no evidence of a reaction between 2 and either C_2H_4 or H_2 was observed.

X-ray Crystallographic Determinations of $Co_2Cp^*_2P_4$ (1) and $Fe_2Cp^*_2P_4$ (2). (a) General Procedures. Intensity data for the two compounds were collected with graphite-monochromated Mo Kα radiation on a Siemens (Nicolet) P3F diffractometer equipped with a liquid-nitrogen cooling apparatus. Crystal alignment and data collection procedures are described elsewhere.[15] Crystal data, data-collection paramters, and least-squares refinement parameters for each structure are presented in Table I. Cell dimensions and their esd's were obtained from a least-squares analysis of 22 well-centered reflections ($9° < 2\theta < 26°$) for 1 and 13 reflections ($9° < 2\theta < 20°$) for 2. Axial photographs confirmed the approximate lattice lengths and monoclinic symmetries for the respective unit cells. Intensities of three chosen standard reflections for each compound did not vary significantly (<2% for 1; <5% for 2) during the data collections.

The SHELXTL PLUS 4.11 package[16] was used to solve and refine the two structures. Heavy-atom positions were determined by direct methods, and the other non-hydrogen atoms were located from difference Fourier syntheses coupled with least-squares refinement. Atomic scattering factors for neutral atoms were used together with anomalous dispersion corrections for all non-hydrogen atoms. An empirical ψ-scan absorption correction was applied to the intensity data of 1; no absorption correction was deemed necessary for 2. Hydrogen atoms for the methyl substituents of the Cp* ligands of 1 and 2 were inserted at idealized positions with an assigned isotropic thermal parameter and were included as fixed contributors in the final stages of refinement.

Table II presents selected interatomic distances and bond angles for 1. Specific interatomic distances are not presented for 2 because of the extensive crystal disorder exhibited by the dimeric

Table I. Crystal, Data-Collection, and Structural Refinement Parameters for $Co_2Cp^*_2P_4$ (1) and $Fe_2Cp^*_2P_4$ (2)

	1	2
fw	512.2	506.0
cryst system	monoclinic	monoclinic
cell const temp, °C	–100	–70
a, Å	11.404 (3)	13.79 (1)
b, Å	14.464 (3)	14.79 (1)
c, Å	14.271 (3)	17.39 (1)
β, deg	107.48 (2)	104.86 (7)
V, Å^3	2246.1 (9)	3430 (5)
space group	$P2_1/n$	$P2_1/c$
Z	4	6
d_{calcd}, g/cm^3	1.52	1.47
μ, mm^{-1}	1.76	1.55
data-collcn temp, °C	–100	–70
radiation	Mo Kα	Mo Kα
scan mode	ω	ω
scan speed, deg/min	5–29	3–29
scan range, deg	2.0	1.2
2θ limits, deg	4–52	3–40
no. of data collcd	4830	3509
cutoff for obsd data	$\|F\| > 3\sigma(F)$	$\|F\| > 3\sigma(F)$
no. of ind obsd data	1909	1485
data/param	8/1	8/1
wght	0.0016 (fixed)	0.0016 (fixed)
goodness-of-fit, GOF	1.23	1.83
$R_1(F)$, $R_2(F)$, %	6.29, 7.43	12.30, 13.55

Table II. Selected Interatomic Distances and Bond Angles for $Co_2Cp^*_2P_4$ (1)

Interatomic Distances (Å)			
P(1)–P(2)	2.053 (4)	P(3)–P(4)	2.058 (4)
Co(1)–P(1)	2.304 (3)	Co(1)–P(2)	2.307 (4)
Co(1)–P(3)	2.303 (3)	Co(1)–P(4)	2.301 (4)
Co(2)–P(1)	2.309 (4)	Co(2)–P(2)	2.309 (3)
Co(2)–P(3)	2.303 (4)	Co(2)–P(4)	2.305 (3)
Co(1)···Co(2)	3.102 (3)	P(1)···P(3)	2.737 (4)
P(2)···P(4)	2.705 (4)		
Co(1)–C(1)	2.073 (14)	Co(1)–C(2)	2.081 (15)
Co(1)–C(3)	2.083 (11)	Co(1)–C(4)	2.077 (11)
Co(1)–C(5)	2.089 (12)	Co(2)–C(11)	2.069 (11)
Co(2)–C(12)	2.074 (11)	Co(2)–C(13)	2.058 (12)
Co(2)–C(14)	2.061 (12)	Co(2)–C(15)	2.082 (13)
C(1)–C(2)	1.386 (17)	C(1)–C(5)	1.409 (15)
C(1)–C(6)	1.531 (17)	C(2)–C(3)	1.420 (15)
C(2)–C(7)	1.525 (16)	C(3)–C(4)	1.429 (14)
C(3)–C(8)	1.500 (15)	C(4)–C(5)	1.427 (14)
C(4)–C(9)	1.505 (14)	C(5)–C(10)	1.484 (15)
C(11)–C(12)	1.431 (14)	C(11)–C(15)	1.448 (14)
C(11)–C(16)	1.486 (14)	C(12)–C(13)	1.431 (14)
C(12)–C(17)	1.492 (14)	C(13)–C(14)	1.407 (15)
C(13)–C(18)	1.531 (15)	C(14)–C(15)	1.417 (15)
C(14)–C(19)	1.537 (14)	C(15)–C(20)	1.497 (16)
Bond Angles (deg)			
P(1)–Co(1)–P(2)	52.9 (1)	P(1)–Co(1)–P(3)	72.9 (1)
P(2)–Co(1)–P(3)	95.5 (1)	P(1)–Co(1)–P(4)	95.5 (1)
P(2)–Co(1)–P(4)	71.9 (1)	P(3)–Co(1)–P(4)	53.1 (1)
P(1)–Co(2)–P(2)	52.8 (1)	P(1)–Co(2)–P(3)	72.8 (1)
P(2)–Co(2)–P(3)	95.4 (1)	P(1)–Co(2)–P(4)	95.3 (1)
P(2)–Co(2)–P(4)	71.8 (1)	P(3)–Co(2)–P(4)	53.1 (1)
Co(1)–P(1)–Co(2)	84.5 (1)	Co(1)–P(1)–P(2)	63.7 (1)
Co(2)–P(1)–P(2)	63.6 (1)	Co(1)–P(2)–Co(2)	84.4 (1)
Co(1)–P(2)–P(1)	63.5 (1)	Co(2)–P(2)–P(1)	63.6 (1)
Co(1)–P(3)–Co(2)	84.7 (1)	Co(1)–P(3)–P(4)	63.4 (1)
Co(2)–P(3)–P(4)	63.5 (1)	Co(1)–P(4)–Co(2)	84.7 (1)
Co(1)–P(4)–P(3)	63.5 (1)	Co(2)–P(4)–P(3)	63.4 (1)

(14) (a) Scherer, O. J.; Brück, T. *Angew. Chem. Int. Ed. Engl.* **1987**, *26*, 59. (b) Scherer, O. J.; Brück, T.; Wolmershäuser, G. *Chem. Ber.* **1989**, *122*, 2049.

(15) Byers, L. R.; Dahl, L. F. *Inorg. Chem.* **1980**, *19*, 277.

(16) SHELXTL PLUS 4.11. Siemens Analytical X-Ray Instruments, Inc., 600 Enterprise Lane, Madison, WI 53719-1173.

units (vide infra). Tables of interatomic distances for **2** (with all distances involving the labeled phosphorus atoms based on the partially occupied positions), positional coordinates for the non-hydrogen atoms, idealized positional and thermal parameters for the hydrogen atoms, anisotropic thermal parameters for all appropriate non-hydrogen atoms, and observed and calculated structure factor amplitudes for each compound ar available as supplementary material.

(b) $Co_2Cp^*_2P_4$ (1). A pale purple parallelepiped-shaped crystal (0.55 × 0.40 × 0.20 mm) of **1** suitable for single-crystal X-ray analysis was grown by a slow, layered diffusion of hexane into a saturated THF solution of the compound. All non-hydrogen atoms were refined anisotropically with no positional or thermal constraints applied. A final electron-density difference map showed no abnormal residual electron density (<1.0/e/Å^3).

(c) $Fe_2Cp^*_2P_4$ (2). Crystals were grown from a slow, layered diffusion of hexane into a saturated CH_2Cl_2 solution of **2**. Most of the translucent brown crystals were either too small for adequate data collection or were badly split. A weakly diffracting, irregularly shaped crystal of approximate dimensions 0.15 × 0.25 × 0.35 mm was selected for data collection and mounted in an argon-filled Lindemann glass capillary.

The crystal structure of **2** presents several unusual and troublesome features. With $Z = 6$, the monoclinic unit cell ($P2_1/c$), contains one 4-fold general set of symmetry-equivalent molecules with C_1-1 site symmetry and one 2-fold special set of symmetry-equivalent molecules with C_i-$\bar{1}$ site symmetry. Both dimeric molecules exhibit rotational disorder about the Fe–Fe bond axis in the crystal. Thus, the positions of the bridging phosphorus atoms are averaged over a number of crystallographic positions. Due to the weakly diffracting crystal, the number of observed data was too small to fully model this extensive disorder. The procedures used to refine the positions and site occupancy values of the phosphorus atoms of **2** are as follows: once the number of phosphorus atoms was unabiguously established as 4 per dimeric unit (vide infra), the larger electron densities located at appropriate distances and orientations from the iron atoms were assigned to phosphorus atoms. The isotropic U values for these atom positions were initially held at approximately 1.2–1.4 times the value for their coordinated iron atoms; their specific site occupancies were then allowed to vary such that the total site occupancy for the phosphorus atoms converged at a value near 4 for the entire independent molecule of C_1 symmetry and near 2 for the half-independent molecule of C_i symmetry. This procedure resulted in a horseshoe-shaped composite of five major peaks with site occupancy factors of approximately 0.5, 1, 1, 1, and 0.5 for the molecule of C_1 symmetry and a hexagonal array of six major peaks (three independent) with refined site occupancy factors of 0.65, 0.58, and 0.77 for the molecule of C_i symmetry. These occupancy values were then fixed, and the anisotropic thermal parameters were allowed to vary independently. This method of anisotropic thermal refinement of the electron-density peaks gave more satifatory results than an isotropic refinement of crystal-disordered rigid P_2 groups. The iron atoms were also refined anisotropically. The Cp* ring carbon atoms were constrained to D_{5h} symmetry with a fixed C–C bond distance of 1.42 Å in order to reduce the number of refinement parameters. While the data/parameter ratio at this point was too low to justify an anisotropic refinement of all atoms, attempted anisotropic refinement of the methyl carbon atoms of the three independent Cp* rings revealed that they also exhibited extensive rotational crystallographic disorder. Consequently, all carbon atoms were refined isotropically. A final Fourier difference map, which exhibited maximum residual electron-density peaks of <1.0 e/Å^3, did not reveal any unusual features.

Results and Discussion

Crystal and Molecular Structural Features of $Co_2Cp^*_2P_4$ (1) and $Fe_2Cp^*_2P_4$ (2). (a) $Co_2Cp^*_2P_4$ (1). The monoclinic unit cell ($P2_1/n$) of **1** contains four crystallographically related, discrete molecules which pack with no unusually short intermolecular distances. The independent molecule has crystallographic C_1-1 site symmetry, but its Co_2P_4 core possesses pseudo-D_{2h} symmetry which is reduced to C_i symmetry upon inclusion of the two staggered Cp* rings. Figure 1 presents the labeling of the primary atoms of **1**. The two P–P bond lengths of 2.053 (4) and 2.058 (4) Å are similar to P–P distances found in μ_2-P_2 ligands in analogous complexes;[4,17] the two P···P nonbonding distances between the two ligands are 2.705 (4) and 2.737 (4) Å (mean = 2.72 Å). The mean of 2.39 Å for the four P–P bonding and nonbonding distances is virtually identical to the average P–P distance of 2.38 Å that Scherer et al.[4] reported for the proposed rectangular *cyclo*-P_4 units of the (tetramethylethylcyclopentadienyl)-cobalt dimer.

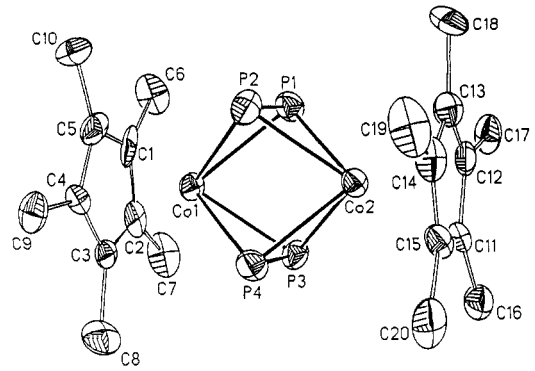

Figure 1. Molecular configuration of $Co_2Cp^*_2(\mu_2\text{-}\eta^2\text{-}P_2)_2$ (**1**), which possesses C_1-1 crystallographic symmetry but exhibits pseudo-C_i-$\bar{1}$ symmetry. The Co_2P_4 core ideally conforms to D_{2h} symmetry. Atomic thermal ellipsoids are drawn at the 30% probability level. The molecular configuration of $Fe_2Cp^*_2(\mu_2\text{-}\eta^2\text{-}P_2)_2$ (**2**), in which the two centrosymmetrically related FeCp* moieties were clearly resolved from the X-ray crystallographic determination but not the bridging P_2 ligands due to a rotational-type crystal disorder, is presumed to be similar to that of **1** (except for an electron-pair bonding distance (2.59 Å) in **2** versus a nonbonding one (3.10 Å) in **1**).

These two η^2-coordinated P_2 ligands which link two CoCp* fragments at a Co···Co nonbonding distance of 3.102 (3) Å are coplanar. The eight experimentally equivalent, independent Co–P bonding distances vary from 2.301 (4) to 2.309 (4) Å. The least-squares plane defined by the two μ_2-P_2 units and the planes of the two Cp* rings are parallel within 1°.

(b) $Fe_2Cp^*_2P_4$ (2). The monoclinic cell ($P2_1/c$) of **2** contains six molecules, of which four symmetry-related molecules lie in general 4-fold positions and two symmetry-related molecules lie on centers of symmetry. These six molecules per cell pack with no abnormal intermolecular interactions.

The iron dimer with C_1 crystallographic site symmetry has a normal Fe–Fe single-bond distance of 2.585 (6) Å. The five composite electron-density peaks for the crystal-disordered phosphorus atoms (Fe–P(av) = 2.29 Å) are virtually coplanar, and the two eclipsed Cp* rings (Fe–C(av) = 2.10 Å) are each tilted approximately 10° away from this plane to give an idealized molecular geometry of C_s-m. The iron dimer generated from the half-independent fragment with C_i site symmetry has a similar electron-pair Fe–Fe bonding distance of 2.591 (11) Å. The mean plane defined by the six electron-density peaks of the crystal-disordered phosphorus atoms (Fe–P(av) = 2.38 Å) and the mean plane of the carbon atoms of the Cp* ring (Fe–C(av) = 2.07 Å) of the independent half-molecule are parallel within 1°. The two crystallographically discrete sets of molecules are oriented nearly orthogonally to each other,

(17) (a) Goh, L. Y.; Chu, C. K.; Wong, R. C. S.; Hambley, T. W. *J. Chem. Soc., Dalton Trans.* **1989**, 1951. (b) Campana, C. F.; Vizi-Orosz, A.; Pályi, L.; Markó, L.; Dahl, L. F. *Inorg. Chem.* **1979**, *18*, 3054.

(18) Reference deleted on revision.

with the planes defined by their phosphorus atoms differing by 85.0°.

Bonding Analysis of $Co_2Cp^*_2P_4$ (1) and $Fe_2Cp^*_2P_4$ (2). The μ_2-η^2-P_2 ligands of **1** are each formal 4-electron donors[3b] to the two 14-electron CoCp* fragments. Thus, the dimeric unit attains a 36 valence electron count, which is in accordance with the observed nonbonding Co···Co distance. Under the assumption that the four phosphorus atoms in **2** are similarly coordinated to the two iron atoms as μ_2-η^2-P_2 ligands, an 18-electron count is achieved for each iron atom upon the formation of an Fe–Fe single bond between the two 13-electron FeCp* fragments. The resultant 34 valence electron count for **2**, which is also found for other dimers containing formal metal–metal single bonds, is consistent with the Fe–Fe bond length observed for each dimer.

Spectral–Electrochemical Properties of $Co_2Cp^*_2P_4$ (1) and $Fe_2Cp^*_2P_4$ (2). (a) Mass Spectral Analysis. The mass spectra provide a substantiation of the composition of **1**, as derived from its single-crystal X-ray data. Additionally, they provide crucial information concerning the elemental composition of the crystallographically disordered iron dimer (**2**) and convincing evidence that the phosphorus atoms of **2** are coordinated analogously to those of **1**.[9]

The parent-ion peak ($[M]^{+,-}$) for **1** appears in both the positive- and negative-ion mass spectra. However, less abundant, higher mass peaks assigned to $[M + P]^{+,-}$ (viz., $[Co_2Cp^*_2P_5]^{+,-}$) and $[M + P - Me]^{+,-}$ are also detected. Positive- and negative-ion LD/FT mass spectra of **2** reveal much larger parent-ion peaks (both 100% abundant) and relatively smaller fragment-ion peaks than those of **1**. This observation is consistent with the existence of direct metal–metal bonding only in the iron dimer. The dominant parent-ion peak for **1** shows conclusively that four phosphorus atoms are present in each dimeric unit. The close similarity of the daughter-ion fragmentation patterns detected in the positive-ion spectra of **1** and **2** is completely in accordance with the iron dimer (**2**) being structurally analogous to the crystallographically proven cobalt dimer (**1**), which possesses four bridging phosphorus atoms with connectivities corresponding to two discrete μ_2-P_2 units. The corresponding iron/cobalt fragment-ion peaks for some of the more abundant ions observed in their positive-ion spectra are $[M]^+$ at m/z 506/512, $[M - Me]^+$ at m/z 491/497, $[M - P]^+$ at m/z 475/481, $[M - 2P]^+$ at m/z 444/450, and $[Cp^*_2Fe]^+/[Cp^*_2Co]^+$ at m/z 326/329. In fact, the only significant ion peak observed for **2** which is not analogous to any detected in the mass spectra of **1** is the negative-ion peak at m/z 315 (8%) assigned to the fragment $[FeCp^*P_4]^-$. A table listing assigned ion peaks with relative abundances is available as supplementary material.

(b) NMR Spectral Analysis. A ^{31}P NMR spectrum (109.3 MHz; $CDCl_3$; 300 K; H_3PO_4 ext) of **1** shows a broad singlet ($w_{1/2}$ = 30 Hz) at δ −6.06 ppm in accordance with the pseudo-D_{2h} symmetry of the Co_2P_4 core. An analogous ^{31}P NMR spectrum (109.3 MHz; $CDCl_3$; 300 K; H_3PO_4 ext), consisting of a broad singlet ($w_{1/2}$ = 38 Hz) at δ 126.58 ppm, is found for **2**. The singlet is consistent with the Fe_2P_4 core of **2** also having pseudo-D_{2h} symmetry as found in **1**.

(c) Electrochemical Analysis. Cyclic voltammograms for **1** and **2** show that each dimer exhibits reversible redox behavior in CH_2Cl_2 within the observed range of +1.8 to −2.0 V (200 mV/s). **1** undergoes one reversible oxidation ($E_{1/2}$ = 0.244 V, ΔE_p = 0.131 V), followed closely by an irreversible oxidation at E_p = 0.55 V. **2** exhibits a reversible oxidation at $E_{1/2}$ = 0.087 V (ΔE_p = 0.076 V) and an irreversible reduction at ca. −1.7 V.

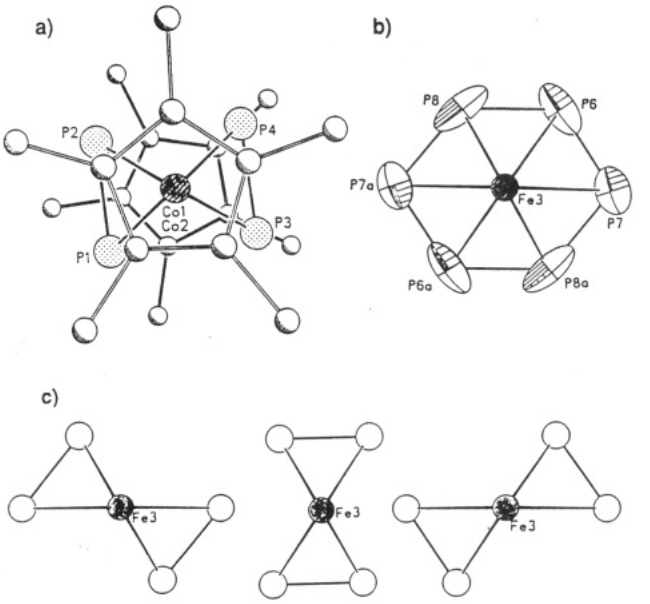

Figure 2. (a) End-on view of $Co_2Cp^*_2(\mu_2$-η^2-$P_2)_2$ (**1**) with pseudo-C_i-$\bar{1}$ symmetry. (b) Anisotropic thermal ellipsoids for the six composite electron-density maxima associated with the bridging tetraphosphorus fragment in the crystal-disordered $Fe_2Cp^*_2$-$(\mu_2$-η^2-$P_2)_2$ (**2**) of crystallographic C_i-$\bar{1}$ site symmetry. These six phosphorus density maxima in **2** can be readily interpreted in terms of a 3-fold rotational disorder about the Fe–Fe bond involving the superposition of three equally populated orientations of the rectangularly oriented μ_2-P_2 ligands as shown in (c).

Structural Analyis of the Tetraphosphorus Connectivities in $Fe_2Cp^*_2P_4$ (2). Single-crystal X-ray diffraction, ^{31}P NMR, and LD/FT mass spectral analysis all contribute to the formulation of **2** as $Fe_2Cp^*_2(\mu_2$-η^2-$P_2)_2$. The mass spectral data conclusively show that the dimer contains four phosphorus atoms, and the X-ray crystallographic study shows that the electron-density peaks of these crystal-disordered phosphorus atoms are located as dimetal-bridging ligands midway between the metal atoms in a coplanar arrangement. The average Fe–P distances of 2.29 and 2.38 Å and the Fe–Fe bonding distances of 2.585 (6) and 2.591 (11) Å found in the C_1 and C_i dimers, respectively, show that the ligand is not *cyclo*-μ_2-η^4-P_4; such long Fe–P distances (even if artificially elongated by the crystal disorder) are incompatible with the geometrical restraints imposed by a hypothetical bridging *cyclo*-P_4 ligand in the presence of an Fe–Fe bond.[19] The single resonance found in the ^{31}P NMR spectrum is inconsistent with a butadienyl-like μ_2-η^4-P_4 ligand because this species would be expected to exhibit a minimum of two distinct resonances. While the possibility that the four phosphorus atoms are coordinated to the two irons as four separate bridging P atoms cannot be eliminated on the basis of spectral data, electron-counting considerations (which assumes that each hypothetical μ_2-P ligand would donate 3 electrons to the two iron atoms to give an inconsistent dimeric electron count of 38) indicate that such a bonding picture is highly unlikely. Furthermore, to the best of our knowledge, there are no reported complexes containing a μ_2-P atom.

Figure 2 illustrates how a crystallographic 3-fold disorder of two rectangularly shaped η^2-P_2 units would produce the

(19) (a) Tremel, W.; Hoffmann, R.; Kertesz, M. *J. Am. Chem. Soc.* **1989**, *111*, 2030. (b) For bonding parameters of *cyclo*-P_4 ligands, see: Scherer, O. J.; Vondung, J.; Wolmershäuser, G. *Angew. Chem., Int. Ed. Engl.* **1989**, *28*, 1355.

hexagonal array of electron-density maxima associated with the three independently observed partial-occupancy positions of the phosphorus atoms in the C_i dimer of **2**. A similar modeling of the five composite electron-density maxima in the C_1 dimer is less easily visualized, but the observed 20° distortion of the dimer from linearity may be due to crystal packing forces which also distort the μ_2-P_2 ligands from their idealized D_{2h} geometry in the solid state.

Conclusions

While other studies have shown that electron-deficient transition-metal fragments readily add as terminal ligands to the nonbonding electron pairs of μ_2-P_2 units,[20] there have been no reports of the addition of metal fragments *across* the P–P bond, with or without P–P bond cleavage. Structural determinations have shown that simple terminal adduct coordination of metal fragments to the unshared electron pairs of a preformed μ_2-P_2 ligand has relatively little effect on the P–P bond length. For example, addition of one or two electrophilic $Cr(CO)_5$ fragments to $Cr_2Cp_2(CO)_4(\mu_2\text{-}P_2)$[20a] results in an alteration of the P–P bond length from 2.060 (1) Å in the parent compound to 2.052 (2) Å in the monoadduct complex and to 2.063 (1) Å in the biadduct $Cr_2Cp_2(CO)_4(\mu_2\text{-}P_2)[Cr(CO)_5]_2$. This stereophysical behavior contrasts sharply with that of the aforementioned $Mo_2Cp''_2(\mu_2\text{-}S_2)(\mu_2\text{-}S)_2$ dimers in which electron-deficient metal fragments prefer to add across the S–S bond or between the two μ_2-S ligands forming metal-bonding triangles and various cubanes.[21] Simple end-on adduct coordination to the unshared electron pairs of the sulfide ligands, in fact, results in relatively unstable complexes.[21a] The ability of a metal-coordinated disulfide ligand to participate in reductive bond-cleavage chemistry, e.g., $(S\text{–}S)^{2-} + 2e^- \rightarrow 2S^{2-}$, is well established,[22] but this avenue appears closed to the μ_2-P_2 ligand, presumably due to its stronger P–P bonding.

Reductive metal–fragment addition across the P–P bond may be facilitated by conversion of the μ_2-P_2 ligand to a μ_2-P_2R_2 ligand. However, the observed difference in reactivity toward electrophilic metal fragments between the diphosphide and disulfide ligands is also observed for the reductive addition of molecular species such as H_2 and C_2H_4. These molecules add readily under mild conditions to the $Mo_2Cp''_2(\mu_2\text{-}S_2)(\mu_2\text{-}S)_2$ dimers.[7b] Although experimental conditions in attempted addition of these molecules to the P_2 units of **1** and **2** were not particularly vigorous (1.4 atm, 25 °C), the absence of any detectable reaction is perhaps indicative of the general inertness of the diphosphide ligand to these molecular reactants.

A sequential electrophilic/nucleophilic process, such as the addition of CH_3^+ (as CH_3I) followed by addition of CH_3^- (as CH_3Li) to $[MoCp(\mu_2\text{-}S)]_2(\mu_2\text{-}S_2CH_2)$,[23] may be a more productive route to formation of μ_2-P_2R_2 ligands than a one-step molecular addition. Although Vahrenkamp and co-workers[24] have found that analogous diiron-complexed μ_2-N_2R_2 ligands are *not* reactive intermediates in the formation of the μ_2-RNCONR ligand, which had been previously hypothesized to originate from CO insertion across the N=N bond, these μ_2-N_2R_2 ligands will coordinate to an additional electron-deficient $Fe(CO)_3$ fragment. The resultant trimetal-coordinated μ_3-N_2R_2 ligand can then undergo thermolytic cleavage to form two capping μ_3-NR groups. These chemical tranformations would appear to provide a promising route for the synthesis of larger metal clusters from bridging diphosphide metal dimers.

Acknowledgment. This research was supported by the National Science Foundation (Grants CHE-8616697 and CHE-9013059). We thank Dr. Bruce Adams (UW—Madison) for his assistance in obtaining the ^{31}P NMR spectra. We are indebted to Dr. Asgeir Bjarnason (Science Institute, University of Iceland, Reykjavik, Iceland) for obtaining the mass spectra with an EXTREL FTMS-2000 laser-desorption mass spectrometer and to EXTREL FTMS (6416 Schroeder Rd, Madison, WI 53711) for the use of their instrument and for their interest in this project.

Registry No. **1**, 125453-97-6; **2**, 136750-29-3; $CoCp^*(CO)_2$, 12129-77-0; $[FeCp^*(CO)_2]_2$, 35344-11-7; P, 7723-14-0; $[CoCp^*(\mu_2\text{-}CO)]_2$, 69657-52-9; $FeCp^*P_5$, 106211-20-5; C_2H_4, 74-85-1; H_2, 1333-74-0.

Supplementary Material Available: Tables listing interatomic distances for **2**, coordinates and isotropic thermal parameters for all atoms of **1** and **2**, anisotropic displacement coefficients for appropriate non-hydrogn atoms of **1** and **2**, and assigned major ion peaks with relative abundances for LD/FT mass spectra of **1** and **2** (8 pages); tables of observed and calculated structure factor amplitudes for **1** and **2** (23 pages). Ordering information is given on any current masthead page.

(20) (a) Goh, L. Y.; Wong, R. C. S.; Mak, T. C. W. *J. Organomet. Chem.* **1989**, *373*, 71. (b) Goh, L. Y.; Wong, R. C. S.; Mak, T. C. W. *J. Organomet. Chem.* **1989**, *364*, 363. (c) Scherer, O. J.; Sitzmann, H.; Wolmershäuser, G. *J. Organomet. Chem.* **1986**, *309*, 77. (d) Scherer, O. J.; Sitzmann, H.; Wolmershäuser, G. *Angew. Chem., Int. Ed. Engl.* **1984**, *23*, 968.

(21) (a) Wachter, J. *Angew. Chem., Int. Ed. Engl.* **1989**, *28*, 1613 and references therein. (b) Brunner, H.; Janietz, N.; Wachter, J.; Zahn, T.; Ziegler, M. L. *Angew. Chem., Int. Ed. Engl.* **1985**, *24*, 133. (c) Cowans, B. A.; Haltiwanger, R. C.; Rakowski DuBois, M. *Organometallics* **1987**, *6*, 995. (d) Cowans, B. A.; Noordik, J.; Rakowski DuBois, M. *Organometallics* **1983**, *2*, 931.

(22) Harmer, M. A.; Halbert, T. R.; Pan, W.-H.; Coyle, C. L.; Cohen, S. A.; Stiefel, E. I. *Polyhedron* **1986**, *5*, 341.

(23) Casewit, C. J.; Haltiwanger, R. C.; Noordik, J.; Rakowski DuBois, M. *Organometallics* **1985**, *4*, 119.

(24) Wucherer, E. J.; Tasi, M.; Hansert, B.; Powell, A. K.; Garland, M. T.; Halet, J.-F.; Saillard J.-Y.; Vahrenkamp, H. *Inorg. Chem.* **1989**, *28*, 3564.